Improved Kelbg potential for correlated Coulomb systems

Improved Kelbg potential for correlated Coulomb systems

A V Filinov[1], **M Bonitz**[1] **and W Ebeling**[2]

[1] Fachbereich Physik, Universität Rostock, Universitätsplatz 3, D-18051 Rostock, Germany
[2] Institut für Physik, Humboldt-Universität Berlin, Invalidenstrasse 110, D-10115 Berlin, Germany

Abstract
Effective two-body potentials for electron–ion plasmas are analysed. Such potentials which have been previously derived by Kelbg and others capture the basic quantum diffraction effects and are exact in the weak coupling limit. Moreover, using path integral Monte Carlo (PIMC) methods, they can be applied to strongly coupled plasmas which include bound states. We investigate the accuracy of the diagonal Kelbg potential (DKP) as well as the off-diagonal Kelbg potential (ODKP) by comparison with accurate numerical solutions of the off-diagonal two-particle Bloch equation. A significant improvement is achieved by correcting the potential value at zero particle separation.

PACS numbers: 05.30.−d, 52.40.−w

1. Introduction

The behaviour of strongly correlated Coulomb systems at high pressure is of growing importance in many fields, including shock and laser plasmas, astrophysics, metals, semiconductors, dusty plasmas, etc. There has been significant progress in recent years in studying these systems analytically and numerically, see, e.g., [1, 2] for an overview. Analytical methods are based on perturbation expansions in the coupling strength and are thus limited to regions of small coupling parameters, $\Gamma < 1$ or $r_s < 1$, where $\Gamma = e^2/(\bar{r}k_BT)$ and $r_s = \bar{r}/a_B$ (a_B is the Bohr radius and $\bar{r}$ the mean interparticle distance). The alternative approaches are numerical simulations such as Monte Carlo or molecular dynamics (MD) which have no limitations with respect to the coupling strengths. However, standard MD is limited to classical systems. Nevertheless it can be extended to weakly degenerate plasmas [3, 4] by replacing the Coulomb potential by effective quantum pair potentials, such as proposed by Kelbg [5], Deutsch [6] and others e.g., [7–9]. However, no rigorous assessment of the accuracy of effective potentials has been reported yet, which is one of the aims of this paper. Similarly, this question is important for path integral Monte Carlo simulations (PIMC).

Here, use of the Trotter formula allows one to map a strongly degenerate and/or strongly coupled system to a weakly correlated nearly classical one which is dominated by pair correlations. This, further, allows one to reduce the many-body problem to a two-particle one which can be solved either exactly or by using quantum pair potentials, e.g., [10, 11]. The latter case is particularly interesting due to the use of analytical potentials which themselves have physical relevance, explicitly containing quantum effects.

In the present work we check the accuracy and the range of applicability of the Kelbg potential for the case of strong two-particle correlations. The discussion of other types of effective potentials goes beyond the scope of this paper. A detailed comparison of the present results with other potentials will be given in a forthcoming publication [19].

2. Diagonal and off-diagonal Kelbg potentials

In the high-temperature limit the N-particle density matrix can be expanded in terms of two-particle, three-particle, etc contributions. If the temperature is sufficiently high, two-particle contributions are dominant. Here, we concentrate on the available analytical solutions of the two-particle problem in the limit of weak coupling. In this case the two-particle Bloch equation can be solved by perturbation theory,

$$\rho_{ij} = \frac{(m_i m_j)^{3/2}}{(2\pi\hbar\beta)^3} \exp\left[-\frac{m_i}{2\hbar^2\beta}(\mathbf{r}_i - \mathbf{r}'_i)^2\right] \exp\left[-\frac{m_j}{2\hbar^2\beta}(\mathbf{r}_j - \mathbf{r}'_j)^2\right] e^{-\beta\Phi^{ij}} \tag{1}$$

where i, j are particle indices, $\rho_{ij} \equiv \rho(\mathbf{r}_i, \mathbf{r}_j, \mathbf{r}'_i, \mathbf{r}'_j; \beta)$, $\beta = 1/k_B T$ and $\Phi^{ij}(\mathbf{r}_i, \mathbf{r}_j, \mathbf{r}'_i, \mathbf{r}'_j; \beta)$ is the off-diagonal two-particle effective potential. In the following we will consider application of this result to Coulomb systems. First-order perturbation theory yields [12]

$$\Phi^{ij}(\mathbf{r}_{ij}, \mathbf{r}'_{ij}, \beta) \equiv e_i e_j \int_0^1 \frac{d\alpha}{d_{ij}(\alpha)} \text{erf}\left(\frac{d_{ij}(\alpha)}{2\lambda_{ij}\sqrt{\alpha(1-\alpha)}}\right) \tag{2}$$

where $d_{ij}(\alpha) = |\alpha\mathbf{r}_{ij} + (1-\alpha)\mathbf{r}'_{ij}|$, erf($x$) is the error function $\text{erf}(x) = \frac{2}{\sqrt{\pi}}\int_0^x dt\, e^{-t^2}$ and $\lambda_{ij}^2 = \frac{\hbar^2\beta}{2\mu_{ij}}$ with $\mu_{ij}^{-1} = m_i^{-1} + m_j^{-1}$. The diagonal element ($\mathbf{r}'_{ij} = \mathbf{r}_{ij} = \mathbf{r}_i - \mathbf{r}_j$) of Φ^{ij} is just the familiar (diagonal) Kelbg potential (DKP), given by

$$\Phi^{ij}(\mathbf{r}_{ij}, \mathbf{r}_{ij}, \beta) = \frac{e_i e_j}{\lambda_{ij} x_{ij}}\left[1 - e^{-x_{ij}^2} + \sqrt{\pi}x_{ij}[1 - \text{erf}(x_{ij})]\right] \tag{3}$$

with $x_{ij} = |\mathbf{r}_{ij}|/\lambda_{ij}$, and we underline that the Kelbg potential is finite at zero distance.

Since the Kelbg potential is obtained by first-order perturbation theory, its application is limited to weak coupling ($\Gamma \lesssim 1$). Our present goal is to improve the Kelbg potential, extending it to strong coupling, and make it possible to describe bound states of an electron–proton pair. The improved Kelbg potential obtained appears to be valid for temperatures well below the hydrogen binding energy.

3. 'Exact' pair density matrix and pair potential

There are various ways of computing the 'exact' off-diagonal pair density matrix. First, one can use a direct eigenfunction expansion of the density matrix and calculate the contributions from bound and continuum states. This method is particularly useful for the types of potentials where analytic expressions for the continuum wavefunctions exist. Other cases require a separate calculation for each matrix element $\rho(\mathbf{r}, \mathbf{r}'; \beta)$ which may not be efficient for numerical simulations with frequent use of the off-diagonal density matrix, such as path integral Monte Carlo. Usually in such type of simulations it is crucial that the off-diagonal density matrix
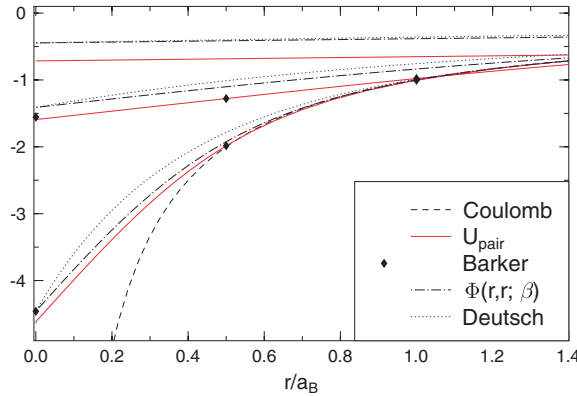
Figure 1. Diagonal effective e–p potentials for several cases: the pure Coulomb potential, the 'exact' pair potential U_p (4), numerical results of Barker [15], the Kelbg potential $\Phi(\mathbf{r}, \mathbf{r}; \beta)$ (3) and the Deutsch potential [6]. Each potential is given at several temperature values (from top to bottom) $T = 10^4$, 10^5 and 10^6 K.

can be quickly evaluated for given initial $(\mathbf{r}_i, \mathbf{r}_j)$ and final $(\mathbf{r}'_i, \mathbf{r}'_j)$ particle positions. In the present work, to solve this problem, we use the *matrix squaring technique* [13, 14]. If the two-particle density matrix is known, the 'exact' quantum pair potential U_p is defined as (d denotes the system dimensionality)

$$\rho(r, r; \beta) \equiv \frac{1}{\lambda_\beta^d} e^{-\beta U_p(r;\beta)} \quad \Rightarrow \quad U_p(r; \beta) = -\frac{1}{\beta} \ln\left[\lambda_\beta^d \rho(r, r; \beta)\right]. \qquad (4)$$

4. Numerical results

In this section we consider application of effective quantum potentials to strongly correlated electron–electron and electron–proton pairs. First, in figure 1 we compare the effective potential obtained using the DKP (3) and U_p (4). Calculation results by Barker obtained from a direct eigenfunction summation [15] and the Deutsch potential [6] are also included. First, we see that the accuracy of the DKP is very good for temperatures $T = 10^6$ K and above. At lower temperatures a systematic offset appears at the origin $r = 0$ which increases with lowering of the temperature. However, we can note that in all cases the DKP goes almost parallel to the 'exact' potential U_p, in particular, it has the same r-derivative at $r = 0$, see [16]. This suggests that a simple correction of the DKP value at $r = 0$ may significantly improve the accuracy, see below.

One can also note that our results for the 'exact' potential U_p agree well with the results of Barker. The comparison with the Deutsch potential shows that it has the same value at $r = 0$ as the Kelbg potential but a different spatial derivative U'_r at the origin, which leads to deviations for $r < a_B$. As can be seen from the figure, these deviations decrease for low temperatures.

Next, in figure 2, we compare the effective potentials (given in units of Ha=2Ry) for electron–electron interaction considering two possible cases of spin projections—triplet (left) and singlet (right) states. It can be seen that spin effects play an important role, being especially relevant at small distances ($r \leqslant a_B$). The value of $U_{ee}^{\uparrow\uparrow}(0)$ is infinite, whereas $U_{ee}^{\uparrow\downarrow}(0)$ remains finite. Even at high temperatures $U_{ee}^{\uparrow\uparrow}$ differs significantly from $U_{ee}^{\uparrow\downarrow}$. At low temperatures it appears as if spin effects become relatively less important, but this is not entirely true. Most
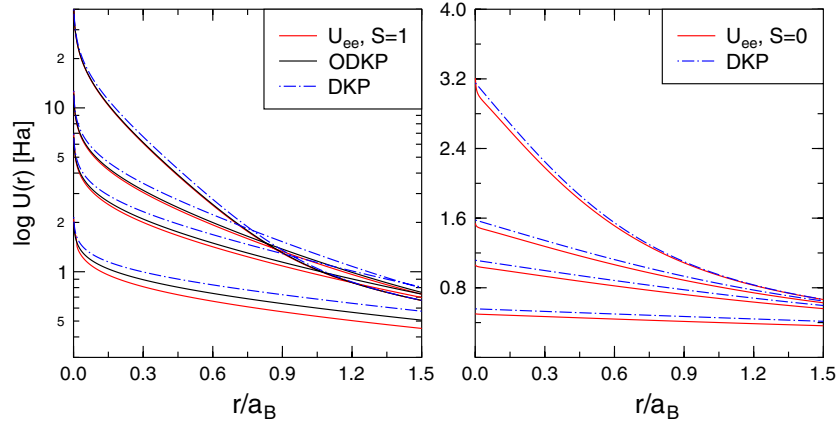
Figure 2. Diagonal effective pair potentials for electron–electron interaction. Left: *parallel spins*, $U_{ee}^{\uparrow\uparrow}(r;\beta)$—'exact' pair potential, ODKP—off-diagonal Kelbg potential, using the antisymmetrical density matrix (6), DKP—using (7). Right: *antiparallel spins*, $U_{ee}^{\uparrow\downarrow}$—'exact' pair potential and DKP. Each potential is given at four temperature values (from bottom to top) $T = 31\,250,\ 125\,000,\ 250\,000$ and 10^6 K.

macroscopic properties depend on $e^{-\beta U}$, and with decreasing temperature the product βU is an increasing function. This means that the importance of the small distance region also increases.

In figure 2 we also present the effective potentials obtained in the Kelbg approximation. First, for the case when the electrons are distinguishable particles the potential $U_{ee}^{\uparrow\downarrow}$ coincides with the DKP (3). One can note that, compared to figure 1, showing the attractive electron–proton potential which contains contributions from the bound states, here (right part of figure 2) the DKP is closer to the 'exact' pair potential.

For parallel spins the coordinate part of the wavefunction (or density matrix) must be antisymmetric, so the effective potential must be defined as

$$e^{-\beta U_{ee}^{\uparrow\uparrow}(r;\beta)} = \rho_A(\mathbf{r}_i, \mathbf{r}_j, \mathbf{r}_i, \mathbf{r}_j; \beta) = \rho(\mathbf{R}, \mathbf{R})\{\rho(\mathbf{r}, \mathbf{r}) - \rho(\mathbf{r}, -\mathbf{r})\} \quad (5)$$

where the two-particle density matrix is factorized into centre of mass and relative components. Taking into account that the free particle density matrix $\rho(\mathbf{R}, \mathbf{R}) = 1$ and using for $\rho(\mathbf{r}, \mathbf{r})$ equation (1), the effective potential for parallel spins reads

$$U_{ee}^{\uparrow\uparrow}(r; \beta) = -\frac{1}{\beta}\ln\left[e^{-\beta\Phi^{ee}(\mathbf{r},\mathbf{r})} - e^{-\frac{4\mu_{ee}}{2\hbar^2\beta}r^2} e^{-\beta\Phi^{ee}(\mathbf{r},-\mathbf{r})}\right]. \quad (6)$$

Here for the off-diagonal density matrix we use the combination of equations (1) and (2). The contribution to exchange comes not only from the kinetic energy part of the density matrix but also from the nondiagonal potential $\Phi^{ij}(\mathbf{r}, -\mathbf{r})$ (2). If one uses the DKP as the diagonal approximation for $\Phi^{ij}(\mathbf{r}, -\mathbf{r})$, then the above expression reduces to

$$U_{ee}^{\uparrow\uparrow}(r; \beta) = \Phi^{ee}(\mathbf{r}, \mathbf{r}) - \frac{1}{\beta}\ln\left[1 - e^{-\frac{4\mu_{ee}}{2\hbar^2\beta}r^2}\right]. \quad (7)$$

For $r \to 0$ this potential shows a logarithmic divergency. In figure 2 the results for these two cases (6) and (7) are given. One can note that the diagonal approximation (7) is less accurate at all temperatures. At $T = 10^6$ K the effective potential (6) practically coincides with the potential U_{ee} obtained from the 'exact' two-particle density matrix.
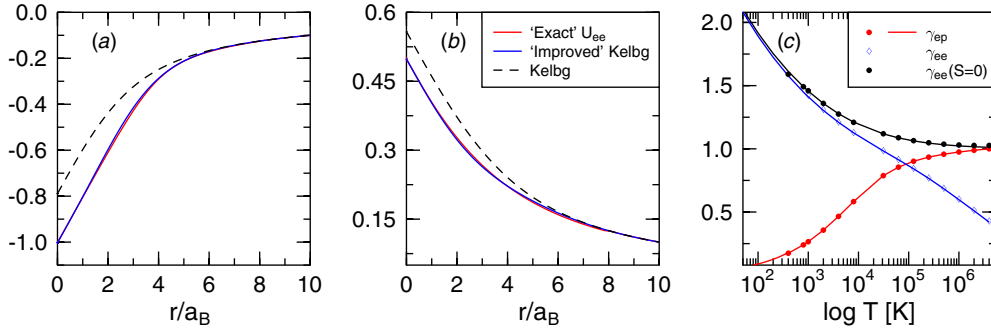
Figure 3. (*a*), (*b*) The original, equation (3), and the improved, equation (8), Kelbg potential versus 'exact' result, equation (4) for $T = 31\,250$ K. (*c*) Fit parameter γ for electron–proton (ep) and electron–electron (ee) interactions as a function of temperature ($\gamma_{ee}(S = 0)$ is for electrons with different spins, γ_{ee} is a spin averaged result).

5. Improved diagonal Kelbg potential

Improved potentials were considered in [17, 18]. In [18] it was suggested that for the free charges the real interactions have the same functional form as the Kelbg potential with an additional free parameter γ_{ij},

$$\tilde{\Phi}(r_{ij}, \beta, \gamma_{ij}) = \frac{e_i e_j}{r_{ij}} \left[1 - e^{-\frac{r_{ij}^2}{\lambda_{ij}^2}} + \sqrt{\pi} \frac{r_{ij}}{\lambda_{ij} \gamma_{ij}} \left(1 - \mathrm{erf}\left[\gamma_{ij} \frac{r_{ij}}{\lambda_{ij}} \right] \right) \right]. \quad (8)$$

This modified potential preserves the correct first derivative, $\tilde{\Phi}(0, \beta)'_r = -\frac{e_i e_j}{\lambda_{ij}^2}$, of the original Kelbg potential (3) but, at the same time, the height of the potential at $r = 0$ is governed by γ_{ij}: $\tilde{\Phi}(r_{ij} = 0, \beta, \gamma_{ij}) = \frac{e_i e_j}{\lambda_{ij} \gamma_{ij}}$. Thus, the parameter γ_{ij} allows us to correct the height of the DKP at $r = 0$ in such a way that the improved Kelbg potential achieves very good quantitative agreement with the 'exact' pair potential U_p in a wide range of temperatures.

In figures 3(*a*) and (*b*) we compare the DKP, improved DKP and 'exact' pair potential U_p for electron–proton (figure 3(*a*)) and electron–electron interactions (figure 3(*b*)). With the additional parameter γ_{ij}, the improved DKP practically coincides with the 'exact' potential even at strong coupling ($T \sim 0.2Ry$) giving a dramatic improvement of the original Kelbg potential, cf figure 1. The temperature dependence of γ_{ij} (figure 3(*c*)) was obtained by fitting the values of $\tilde{\Phi}(r_{ij}, \beta, \gamma_{ij})$ to U_p (4) at $r = 0$. We also show the case γ_{ee} corresponding to results of the fitting procedure applied to the electron potential averaged over spins: $\gamma_{ee} = -\sqrt{\pi}\, e^2 \beta / \lambda_{ee} \ln\left[\frac{1}{2}\left(S_{ee}^{\uparrow\uparrow} + S_{ee}^{\uparrow\downarrow} \right)\big|_{r_{ij}=0} \right]$, where S_{ee} denotes the binary Slater sum for two electrons.

The physical content of figure 3(*c*) is the following: in the limit of high temperatures, both correction parameters γ_{ep} and $\gamma_{ee}(S = 0)$ approach 1, i.e. $\tilde{\Phi}_{ij} \to \Phi_{ij}$, which means that the height of the potential at $r_{ij} = 0$ is determined by the De Broglie wavelength of *free* particles, λ_{ij}.[3] For temperatures below one Rydberg γ_{ij} starts to deviate from 1. The quantum extension of particles is becoming influenced by interaction effects and is now of the order $\tilde{\lambda}_{ij} = \lambda_{ij} \gamma_{ij}$ instead of thermal wavelength λ_{ij} [19].

[3] The analytical form of the Kelbg potential is not well suited to describing the interaction of electrons with parallel spin. Instead, a suitable analytical approximation is given by equation (7).

Consider first the e–p interaction. Here, obviously, for $T \to 0$ the correct potential value is given by the ground state energy of a hydrogen atom, i.e. $\tilde{\Phi}_{ep}(0) \to -e^2/2a_B$. This leads to $\gamma_{ep} \to 2a_B/\lambda_{ep}$, i.e. the effective quantum extension of the electron is given by the Bohr radius. For a pair of electrons, on the other hand, if the temperature is lowered, Coulomb repulsion leads to a growth of the effective quantum wavelength above the De Broglie value, as can be clearly seen in figure 3(*c*). Due to the corrected value of the electron 'size', the improved Kelbg potentials (8) are much closer to the 'exact' expression (4). Most importantly, the potentials (8) are not limited to weak coupling as the original Kelbg potential and are, therefore, of high value for both analytical and computational studies of quantum plasmas. A more detailed analysis will be given in a forthcoming paper.

Acknowledgments

References

[1] Kraeft W D, Kremp D, Ebeling W and Röpke G 1986 *Quantum Statistics of Charged Particle Systems* (Berlin: Akademie-Verlag)
      Kraeft W D, Kremp D, Ebeling W and Röpke G 1988 *Quantum Kinetic Theory* (Leipzig: Teubner)
[2] Bonitz M (ed) 2000 *Progress in Nonequilibrium Greens Functions* (Singapore: World Scientific)
      Bonitz M *et al* 1996 *J. Phys.: Condens. Matter* **8** 6057
      Kwong N H and Bonitz M 2000 *Phys. Rev. Lett.* **84** 1768
[3] Hansen J P and McDonald I R 1981 *Phys. Rev.* A **23** 2041
[4] Golubnychiy V, Bonitz M, Kremp D and Schlanges M 2001 *Phys. Rev.* E **64** 016409 (2002 *Contrib. Plasma. Phys.* **42** 37)
[5] Kelbg G 1963 *Ann. Phys., Lpz* **12** 219
      Kelbg G 1963 *Ann. Phys., Lpz* **13** 354
      Kelbg G 1964 *Ann. Phys., Lpz* **14** 394
[6] Deutsch C 1977 *Phys. Lett.* A **60** 317
[7] Rogers F J 1981 *Phys. Rev.* A **23** 1008
[8] Gombert M-M, Minoo H and Deutsch C 1984 *Phys. Rev.* A **29** 940
[9] Perrot F and Dharma-wardana M W C 2000 *Phys. Rev.* B **62** 16536
[10] Filinov V S, Fortov V E, Bonitz M and Kremp D 2000 *Phys. Lett.* A **274** 228
[11] Filinov V S, Bonitz M, Ebeling W and Fortov V E 2001 *Plasma Phys. Control Fusion* **43** 743
[12] Ebeling W, Hoffmann H J and Kelbg G 1967 *Contrib. Plasma Phys.* **7** 233 and references therein
[13] Storer R G 1968 *J. Math. Phys.* **9** 964
      Klemm A D and Storer R G 1973 *Aust. J. Phys.* **26** 43
[14] Ceperley D M 1995 *Rev. Mod. Phys.* **65** 279
[15] Barker A A 1971 *J. Chem. Phys.* **55** 1751
[16] Rohde K, Kelbg G and Ebeling W 1968 *Ann. Phys., Lpz* **21** 1
[17] Gombert M-M and Minoo H 1989 *Contrib. Plasma Phys.* **29** 355
[18] Wagenknecht H, Ebeling W and Förster A 2001 *Contrib. Plasma Phys.* **41** 15 and references therein
[19] Filinov A V, Bonitz M and Ebeling W to be published